Improving the Creep Stability of High-Density Polyethylene with Acicular Titania Nanoparticles

F. Bondioli,[1] A. Dorigato,[2,3] P. Fabbri,[1,3] M. Messori,[1,3] A. Pegoretti[2,3]

[1]*Department of Materials and Environmental Engineering, University of Modena and Reggio Emilia, Via Vignolese 905/A, 41100 Modena, Italy*
[2]*Department of Materials Engineering and Industrial Technologies, University of Trento, Via Mesiano 77, 38100 Trento, Italy*
[3]*NIPLAB Reference Centre, Italian Interuniversity Consortium on Materials Science and Technology, Florence, Italy*

Received 19 June 2008; accepted 20 October 2008
DOI 10.1002/app.29472
Published online 23 January 2009 in Wiley InterScience (www.interscience.wiley.com).

ABSTRACT: Acicular titania nanoparticles with average dimensions of 15 × 60 nm^2 were produced by hydrothermal crystallization of $TiOCl_2$. Titania particles were surface-functionalized with octadecylsilane to obtain an organophilic surface. High-density polyethylene (HDPE) nanocomposites were prepared by melt compounding with 2, 3, and 5 vol % concentrations of untreated and surface-functionalized titania nanoparticles. Quasi-static mechanical tensile tests evidenced slight increments of both the elastic modulus and stress at yield, which were accompanied by a marked reduction of the strain at break at high filler contents. The introduction of titania nanoparticles induced a substantial reduction of the creep compliance of the HDPE matrix and of its creep rate, especially at long loading times. Untreated titania nanoparticles were more effective in reducing the creep compliance than the functionalized ones. © 2009 Wiley Periodicals, Inc. J Appl Polym Sci 112: 1045–1055, 2009

Key words: creep; mechanical properties; nanocomposites; polyethylene (PE)

INTRODUCTION

During the last decades, rising interest has emerged in the use of inorganic nanoparticles such as silica, titania, alumina, and calcium carbonate as fillers to increase the rigidity and toughness and reduce the creep compliance of various polymeric matrices.[1,2]

The toughening effect induced by inorganic fillers is generally explained as follows: cavitation of the polymer matrix surrounding the rigid inorganic particles can promote extensive shear yielding, thus increasing the energy absorbed in dissipative phenomena.[3] This mechanism can also be observed in nanocomposites, provided that a proper dispersion of the nanofillers is reached and the agglomeration of the nanoparticles is prevented.[4]

In many technological applications, thermoplastic materials are intended to sustain long-lasting constant loads with limited deformation, and in many cases, the poor creep resistance represents a severe limitation.[5,6] Reinforcement with relatively small amounts of nanoparticles has been proven to be a viable solution for reducing the creep compliance of thermoplastic matrices.[1] For example, titania nanoparticles have been proven to markedly reduce the creep compliance of nylon 66,[7–10] whereas alumina nanoparticles effectively reduce the creep compliance of polystyrene.[11] Also, this research group has documented a marked reduction of the creep compliance of high-density polyethylene (HDPE) filled with submicrometer titania particles[12] and organoclays.[13] It is believed that nanoparticles may effectively restrict the motion of polymer chains, influencing the stress transfer at the nanoscale, with positive effects on the final creep stability of the material. Unfortunately, even if a number of methods are available for the evaluation of the stress-transfer ability at a fiber–matrix interface in microcomposites,[14] no methods are currently available for nanocomposites.

HDPE is by far the most widely used thermoplastic polymer because of its combination of low cost, high chemical resistance, and relatively good mechanical properties. One very demanding application for this polymer is the production of pipes and fittings for the transportation of water or gas under pressure, for which creep stability is one of the critical issues. To the best of our knowledge, so far only a few works have been published on the creep characterization of HDPE nanocomposites, and almost all are focused on the use of organoclays.[13,15–17] Nevertheless, because of the relatively high

Correspondence to: A. Pegoretti (alessandro.pegoretti@unitn.it).

hydrophobicity of polyolefins, HDPE is difficult to intercalate in the interlayer space of hydrophilic clays, unless chemical compatibilization is attempted. The addition of polyethylene grafted with maleic anhydride to the polyethylene matrix favors the intercalation/exfoliation process, with significant improvements of the material stiffness, maintaining the ultimate properties at an acceptable level. For example, Ranade et al.[17] reported that the creep compliance of HDPE blown films can be significantly reduced by the introduction of Cloisite 15A clay and maleated polyethylene. Moreover, Pegoretti et al.[13] found that the creep stability of HDPE can be enhanced by the introduction of clay to an extent markedly depending on the viscosity of the polymer matrix, the type of organoclay, and the amount of maleated polyethylene.

In a previous work, we investigated the effects of a 1 vol % concentration of submicrometer titania particles on the tensile mechanical properties of HDPE, obtaining some encouraging results for the reduction of its creep compliance.[12]

In this study, acicular titania nanoparticles were produced by hydrothermal crystallization and used to prepare nanocomposites filled at concentrations of 2, 3, and 5 vol % by melt mixing with an HDPE matrix. The effects of both untreated and silane surface-modified particles on the tensile mechanical response of the composites were investigated. Particular attention was devoted to understanding the creep behavior of the resulting nanocomposites.

EXPERIMENTAL

Materials

Titanium(IV) oxychloride ($TiOCl_2$) and octadecylsilane [$CH_3(CH_2)_{17}SiH_3$], both purchased from Sigma–Aldrich (Milano, Italy), were used as received.

HDPE (commercial-grade Lupolen 5031 LQ 449; density = 0.952 g/cm^3, melting temperature = 131°C, melt flow rate = 6.5 g/10 min at 190°C and 2.16 kg) in the form of a fine powder was obtained from Basell Polyolefins (Ferrara, Italy).

Preparation of the titania nanoparticles

The synthesis of titania nanoparticles was realized, in agreement with the procedure described by Bonamartini Corradi et al.,[18] under hydrothermal conditions with a 0.5 molar solution of $TiOCl_2$. The hydrothermal process was performed at 195°C for 2 h. The obtained nanoparticles were washed several times in double-distilled water to adjust the pH to neutral conditions and subsequently wet-milled with ethanol to reduce hard aggregation. The as-obtained particles were coded TiO_2.

Organic surface modification was performed on TiO_2 powders (0.5 g) previously placed in a gas chromatograph vial and dried overnight at 120°C in an oven. Ten milliliters of a solution of $CH_3(CH_2)_{17}SiH_3$ in toluene was injected into the vial with a syringe (the solution contained 25 mmol of modifier per square meter of TiO_2 surface area).[19] The reaction vessel was left at room temperature for 24 h. The obtained samples were subsequently centrifuged with reagent-grade toluene and acetone to remove any possible trace of unreacted silane and then vacuum-dried at 110°C over 24 h. The surface-modified particles were coded M-TiO_2.

Characterization of the titania nanoparticles

The synthesized titania nanoparticles were analyzed with a computer-assisted conventional Bragg–Brentano diffractometer using Ni-filtered Cu Kα monochromatic radiation (λ = 0.15418 nm; PW3710, Philips, Almelo, The Netherlands). The X-ray diffraction (XRD) patterns were collected at room temperature in a 2θ range of 20–80° with a scanning rate of 0.005°/s and a step size of 0.02°. The particle morphology was examined by transmission electron microscopy (TEM) with a JEM 2010 transmission electron microscope (JEOL, Japan). Specimens were prepared by the dispersion of the as-obtained powders in distilled water and then the placement of a drop of the suspension on a copper grid covered with a transparent polymer followed by drying. To estimate the particle size distribution, image analysis was carried out on TEM micrographs with the Materials Pro module of Image Pro Plus 4.5.1 software.

The specific surface area (SSA) and density of the powders were determined by the Brunauer–Emmett–Teller method (Gemini 2360 apparatus, Micromeritics, Norcross, GA) and by a pycnometer (AccuPyc 1330 apparatus, Micromeritics), respectively.

To determine the efficiency of the surface treatment, elemental analyses were carried out on a Carlo Erba (Milano, Italy) EA 1110 apparatus to determine the carbon content of the modified particles.

Simultaneous thermogravimetry (TG) and differential thermal analysis (DTA) measurements were carried out in static air on an STA 449C instrument (Netzsch, Germany) at 10°C/min in the temperature range of 20–1000°C, and the results were used for the determination of the surface concentration of OH groups according to a literature procedure.[20]

Fourier transform infrared (FTIR) spectroscopy was performed in the attenuated total reflectance mode with an Avatar 330 spectrometer (Thermo Nicolet, Waltham, MA). A minimum of 32 scans with a resolution of 4 cm^{-1} were adopted.

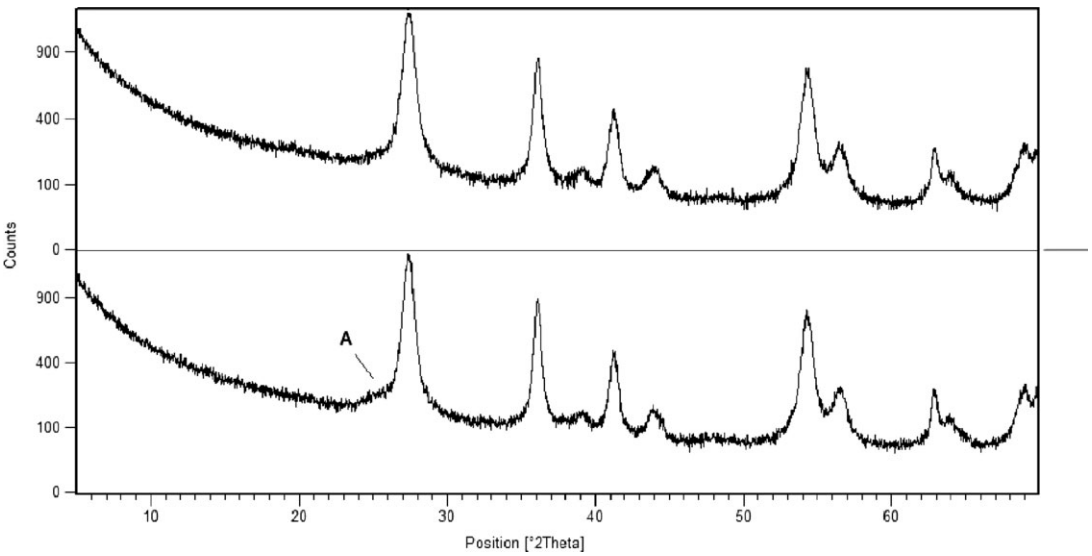

Figure 1 XRD patterns of (upper) TiO_2 and (lower) M-TiO_2 nanoparticles (A = anatase).

Preparation of the composites

Composites were prepared by melt mixing in a Poly-Lab Rheomix R600 internal mixer (Thermo Haake GmbH, Karlsruhe, Germany) equipped with roller rotors and a torque rheometer.

Both HDPE powder and titania nanoparticles were dried at 110°C under a static vacuum overnight before melt mixing. HDPE (ca. 40 g) and titania nanoparticles (2, 3, and 5 vol %) were loaded into the mixing chamber and melt-mixed at 155°C with a rotor speed of 60 rpm. The mixing time was kept equal to 10 min for all samples. The torque was recorded as a function of the mixing time during the melt mixing process to correlate the rheology (melt viscosity) of the composites with the particle content and type. The resulting compound was used to produce sheets with dimensions of 100 × 100 × 1.5 mm^3 by compression molding in a laboratory press (Carver, Inc., USA) operating at 155°C. Depending on the type of titania nanoparticles, the nanocomposites were coded HDPE/TiO_2 x/y or HDPE/M-TiO_2 x/y, where x and y are the volume percentages of the polymer and particles, respectively.

Mechanical characterization of the composites

All mechanical tests were conducted with an Instron (Norwood, MA) 4502 electromechanical universal testing machine equipped with a 1-kN load cell. Dumbbell specimens (ISO 527 type 1BA; gauge length = 30 mm, distance between grips = 55 mm) were punch-cut from the compression-molded sheets and tested in a uniaxial tensile configuration under a constant crosshead speed.

The tensile modulus was determined at a crosshead speed of 0.25 mm/min with an Instron model 2620–601 clip-gauge extensometer (gauge length = 12.5 mm). Because of the large strain involved, yield and fracture parameters were evaluated at a crosshead speed of 50 mm/min without the extensometer. Three specimens were tested for each sample.

Creep tests were conducted on rectangular strips (length = 100 mm, gauge length = 60 mm) punch-cut from the compression-molded sheets. This specimen geometry was selected to avoid problems in determining the actual sample gauge length, and the deformation was then evaluated by the monitoring of the crosshead displacement. After a loading ramp at a crosshead speed of 25 mm/min, a constant nominal stress of 10 MPa was applied for 1 h. Because of the pronounced temperature sensitivity of the creep compliance of HDPE, creep tests were carried out in an Instron model 3119 thermostatic chamber maintained at the constant temperature of 30°C.

RESULTS AND DISCUSSION

Characterization of the titania nanoparticles

XRD patterns of hydrothermally synthesized titania nanopowders are reported in Figure 1. The pattern of the TiO_2 powders (Fig. 1, upper) shows that only the rutile crystalline phase (International Centre for Diffraction Data, source no. 01-087-0920) is detectable. The results of the Rietveld reference intensity ratio refinements, reported elsewhere,[21] confirm that the powders are not completely crystalline with a relevant amount (44 wt %) of an amorphous phase. The morphology of the as-obtained titania powders, observed by TEM analysis, is reported in Figure 2 (left). The analysis shows that obtained primary nanocrystals are composed of acicular particles of the

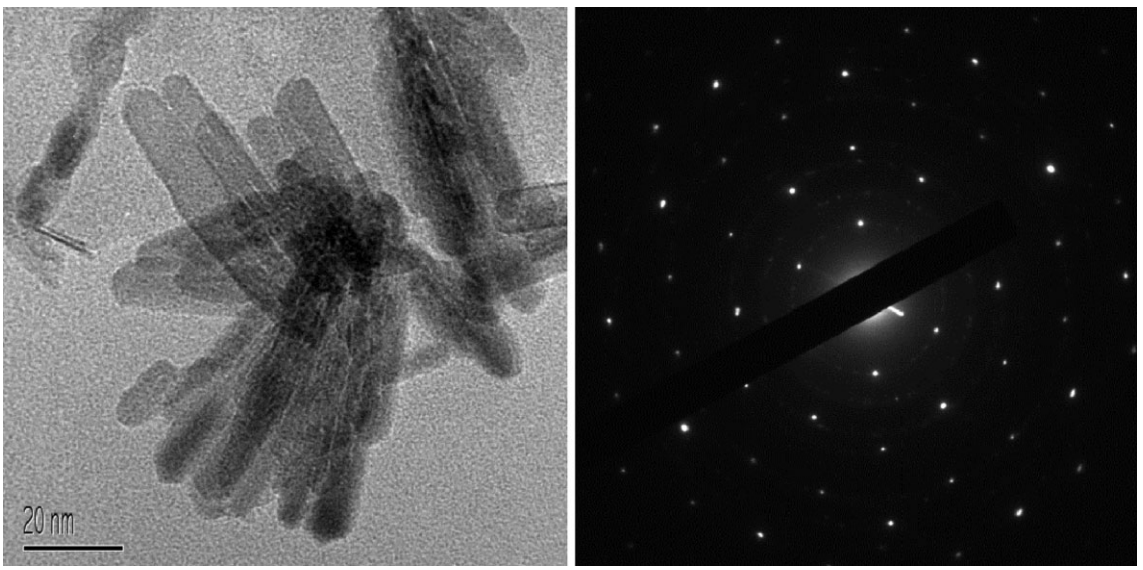

Figure 2 (Left) TEM image and (right) related electron diffraction pattern of the as-obtained titania nanoparticles (TiO_2).

rutile phase (60 nm × 15 nm), as demonstrated by the electronic diffraction pattern (Fig. 2, right). The particles are tightly connected to one another and aggregated into clusters in the range of several hundred nanometers. The XRD pattern of the surface-modified particles (Fig. 1, lower) evidences the presence of a small amount (4.4 wt %) of an anatase phase (International Centre for Diffraction Data, source no. 01-084-1286) that probably crystallized from the amorphous phase during the modification step.

The effectiveness of the surface modification treatment was evaluated by the carbon and hydrogen content (as indicated by elemental analysis) in the surface-modified particles (Table I). Further support is given by the FTIR spectra recorded in the region of the CH_2 vibration, which can be used to investigate the interaction between titania and $CH_3(CH_2)_{17}SiH_3$, as suggested by Helmy and Fadeev.[22] From the spectra reported in Figure 3, the disappearance of the peak related to the Si—H bond [2149.5 cm^{-1}; Fig. 3(c)], together with a significant shift of the peaks related to the surface-modified titania samples [ν_a (asymmetric stretching) = 2918.2 cm^{-1}, ν_s (symmetric stretching) = 2849.7 cm^{-1}; Fig. 3(b)], can be noticed with respect to $CH_3(CH_2)_{17}SiH_3$ [ν_a = 2914.6 cm^{-1}, ν_s = 2847.4 cm^{-1}; Fig. 3(c)], in agreement with the reaction between the reactive surface groups of TiO_2 (presumably Ti—OH groups) and the silane group of octadecylsiloxy and with its attachment as a self-assembled monolayer. Finally, the modification treatment was confirmed by TG/DTA. The DTA curves (Fig. 4) show that, up to 350°C, both materials display similar thermal reactions, even if they are greater with a higher intensity for the surface-treated particles. In particular, an endothermic peak at ~ 100°C, correlated to a significant weight loss, can be attributed to the desorption of water molecules, whereas a diffuse exothermic peak at ~ 320°C, accompanied by a weight loss, can be related to the decomposition of the hydroxyl groups associated with anatase crystallization. On the other hand, M-TiO_2 powders showed a peculiar exothermal event at about 400°C that could be related to the degradation of the surface coating. No weight loss in the powders was observed under heating at higher temperatures, and this indicated no compositional changes. Furthermore, TG/DTA shows that the surface OH group concentration decreases from

TABLE I
Properties of the TiO_2 and M-TiO_2 Powders

Material	SSA (m^2/g)	Average size measured by TEM (nm)[a]	Surface OH concentration (mmol/g)	C content (wt %)	H content (wt %)
TiO_2	108	60 ± 20 13 ± 4	4.1	—	—
M-TiO_2	19	62 ± 15 13 ± 5	2.2	5.03	1.46

[a] Length and diameter of the rodlike particles.

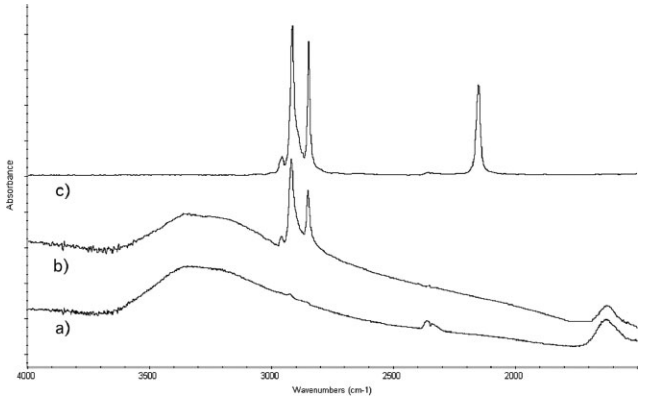

Figure 3 FTIR spectra of (a) TiO_2, (b) M-TiO_2, and (c) $CH_3(CH_2)_{17}SiH_3$.

4.1 mmol/g for TiO_2 to 2.2 mmol/g for M-TiO_2 (Table I) according to the reaction between $CH_3(CH_2)_{17}SiH_3$ and bare titania particles.

The average particle size as obtained from TEM images (Table I) shows that the modification treatment does not affect the grain size distribution, whereas the significant reduction of SSA after surface treatment with $CH_3(CH_2)_{17}SiH_3$ could be explained by the presence of a former porous structure of the native particles that is partially filled by the surface coating.

Characterization of the composites

Melt viscosity

The expected improvement in the mechanical properties derived from the introduction of a rigid phase (filler/reinforcing agent) into the polymer matrix is usually accompanied by an increase in the melt viscosity. The higher melt viscosity represents a disadvantage for processing techniques such as extrusion and injection molding, although it can be beneficial for film extrusion.

To gain some information about the melt viscosity of the composites investigated in this study, the torque values were recorded immediately before the end of the run. These data are reported in Figure 5

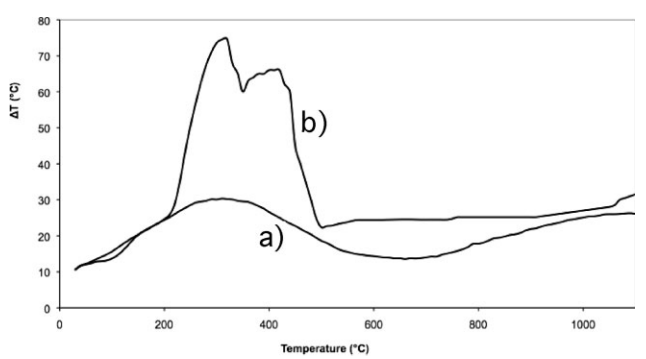

Figure 4 DTA curves of (a) TiO_2 and (b) M-TiO_2.

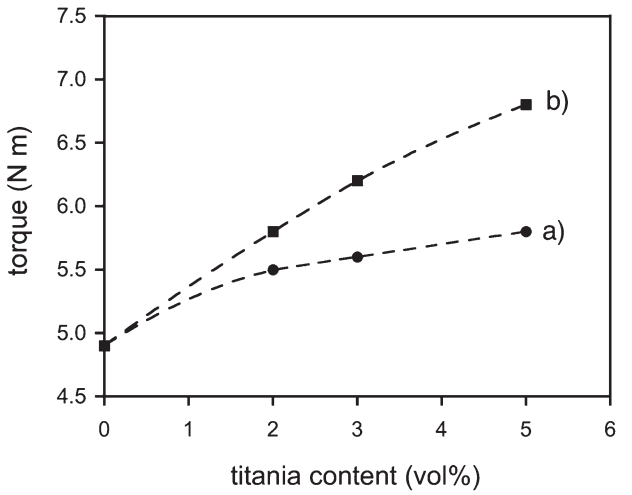

Figure 5 Torque values recorded during the melt mixing of nanocomposites containing various amounts of (a) TiO_2 and (b) M-TiO_2 nanoparticles.

and indicate that the presence of nanoparticles affects the rheology with respect to the pure polymer. In particular, the torque evaluated at 10 min, that is, at the end of the melt-mixing process, increases from 4.9 N m for pure HDPE to 5.5–5.8 N m for the polymer filled with unmodified particles (from 98/2 HDPE/TiO_2 to 95/5 HDPE/TiO_2) and to 5.8–6.8 N m for the polymer filled with surface-modified particles (from 98/2 HDPE/M-TiO_2 to 95/5 HDPE/M-TiO_2). As expected, all composites exhibited an increased melt viscosity because of the presence of a rigid filler, as the general rules for filled polymer melts claim.[23] A somewhat higher melt viscosity was always obtained in the case of surface-modified particles with respect to the pristine ones. This behavior could be considered a preliminary indication of an improved interaction related to somewhat better dispersion of surface-modified nanoparticles in the polymer melt.[24,25]

Quasi-static tensile tests

An example of the characteristic instrumented tensile stress–strain curves at small deformation levels is reported in Figure 6. A pronounced nonlinear behavior can be noticed even at very low strain levels. This behavior is commonly encountered for polymeric materials with a pronounced viscoelastic response, such as many thermoplastics, particularly partially crystalline ones.[26] Consequently, according to the ISO 527 standard, the elastic modulus was evaluated as a secant value between the strain limits of 0.05 and 0.25%.

The tensile modulus values are listed in Table II. A stiffening effect can be quantified as follows:

$$\Delta E/E_m = (E_c - E_m)/E_m \quad (1)$$

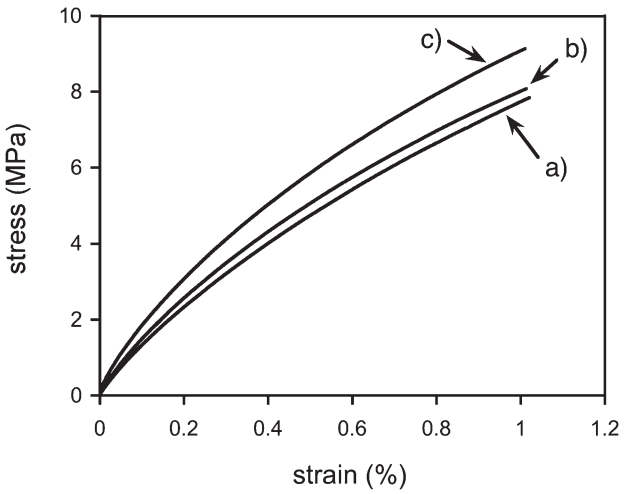

Figure 6 Representative stress–strain curves at 0.25 mm/min in the small-strain region for (a) HDPE, (b) 95/5 HDPE/TiO_2, and (c) 95/5 HDPE/TiO_2.

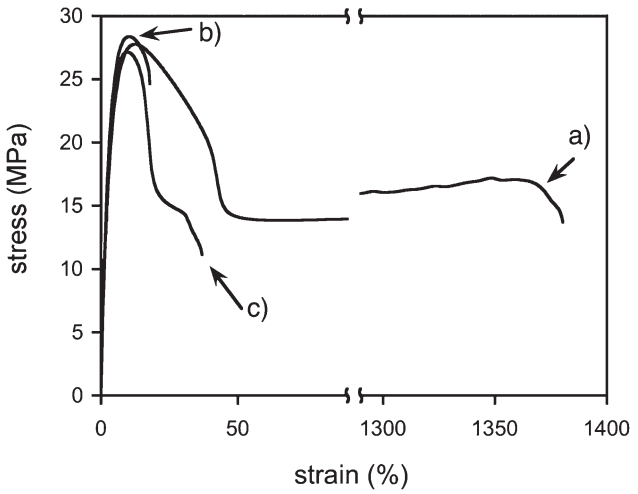

Figure 7 Representative stress–strain curves at 50 mm/min up to fracture for (a) HDPE, (b) 95/5 HDPE/TiO_2, and (c) 95/5 HDPE/M-TiO_2.

where E is the elastic modulus and E_c and E_m are the composite and matrix moduli, respectively. It is possible to observe that the addition of titania nanoparticles generally leads to a stiffening of the HDPE matrix. For the samples filled with untreated nanoparticles, the elastic modulus increases with the filler content, whereas with M-TiO_2, a maximum for the 3 vol % sample, followed by a marked decrease, can be detected. This behavior can be explained if we consider that the surface modification promotes the filler–matrix interaction, but for high amounts of TiO_2, the presence of an organic interphase, presumably softer than the HDPE matrix, has a detrimental effect on the elastic properties of the material.

The presence of titania nanoparticles also markedly affects the yield and fracture behavior of the HDPE matrix. Representative tensile stress–strain curves at high deformation levels are reported in Figure 7. It is evident that the addition of titania nanoparticles slightly improves the yield strength and dramatically reduces the strain at break values. A summary of the ultimate properties of the investigated composites is reported in Table III. Similar effects were recently observed on the same HDPE matrix filled with an organomodified clay at a concentration of 2 wt %.[13] In polymer/clay nanocomposites, even a small enhancement of the yield strength is generally regarded as an indication of a strong filler–matrix interaction.[17,27–29]

Creep tensile tests

The strain in isothermal tensile creep [$\varepsilon(t,\sigma)$], depending on the time (t) and stress (σ), is usually viewed as consisting of three components,[30–32] including (1) an elastic component [$\varepsilon_e(\sigma)$; instantaneous and reversible], (2) a viscoelastic component [$\varepsilon_{ve}(t,s)$; time-dependent and reversible], and (3) a plastic component [$\varepsilon_p(t,\sigma)$; irreversible]:

$$\varepsilon(t,\sigma) = \varepsilon_e(\sigma) + \varepsilon_{ve}(t,\sigma) + \varepsilon_p(t,\sigma) \quad (2)$$

In the linear viscoelastic region, the magnitude of the three components is linearly proportional to the magnitude of the applied stress, so that the creep compliance [$D(t) = \varepsilon(t,\sigma)/\sigma$] can be defined as a function of time only. Moreover, if no plastic deformation is produced in the course of the creep test, the tensile compliance for the isothermal creep can be expressed as reported in eq. (3):

TABLE II
Elastic Modulus Values of the HDPE and Related Nanocomposites

Material	E (MPa)	$\Delta E/E_m$ (%)
HDPE	1097 ± 71	0.0
98/2 HDPE/TiO_2	1162 ± 64	5.9
97/3 HDPE/TiO_2	1174 ± 19	7.0
95/5 HDPE/TiO_2	1260 ± 67	14.9
98/2 HDPE/M-TiO_2	1183 ± 17	7.8
97/3 HDPE/M-TiO_2	1234 ± 22	12.5
95/5 HDPE/M-TiO_2	1148 ± 90	4.6

TABLE III
Stress at Yield (σ_y) and Deformation at Break (ε_r) of the HDPE and Related Nanocomposites

Material	σ_y (MPa)	ε_r (%)
HDPE	27.7 ± 0.3	1026 ± 531
98/2 HDPE/TiO_2	28.1 ± 0.1	164 ± 46
97/3 HDPE/TiO_2	28.2 ± 0.9	263 ± 177
95/5 HDPE/TiO_2	28.4 ± 0.4	17 ± 5
98/2 HDPE/M-TiO_2	27.8 ± 0.6	225 ± 204
97/3 HDPE/M-TiO_2	28.0 ± 0.2	125 ± 104
95/5 HDPE/M-TiO_2	27.2 ± 0.1	42 ± 8

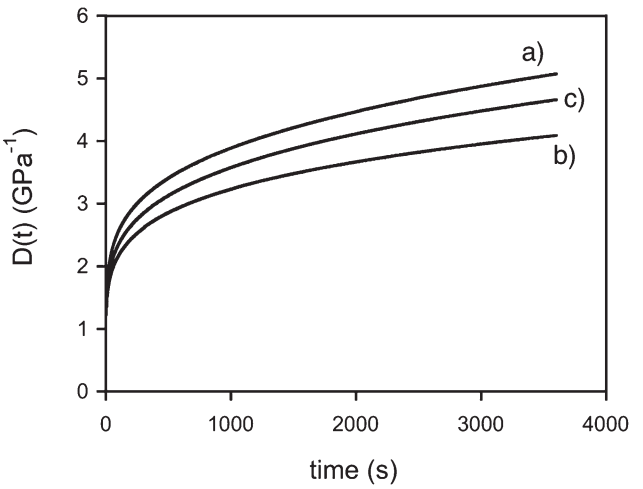

Figure 8 Representative curves of the creep tests for (a) HDPE, (b) 95/5 HDPE/TiO_2 and (c) 95/5 HDPE/M-TiO_2.

$$D(t) = D_e + D_{ve}(t) \quad (3)$$

where D_e and $D_{ve}(t)$ are the elastic and viscoelastic components of the creep compliance, respectively.

In the current study, eq. (3) was used to analyze the experimental data. In fact, all the experiments were performed under the same applied stress to avoid nonlinearity effects. Moreover, the specimens recovered their initial length after unloading, and this excluded the presence of plastic deformations.

Representative creep compliance curves for pure HDPE and HDPE–titania nanocomposites are reported in Figure 8. It is evident that both untreated and surface-modified titania nanoparticles can markedly reduce the creep compliance of the selected HDPE matrix. It also clearly emerges that untreated nanoparticles are more efficient in reducing the creep compliance of the HDPE matrix than the surface-treated ones. This observation is consistent with the behavior under quasi-static tensile tests and in good accordance with the results recently reported for the creep behavior of the same HDPE matrix filled with both untreated and $CH_3(CH_2)_{17}SiH_3$-surface-modified submicrometer titania particles:[12] better creep stability is reported for the composites with untreated particles versus those prepared with the treated particles. Therefore, this result could be explained by the assumption of a somewhat higher compliance of the filler–HDPE interphase when surface-treated titania nanoparticle are used. A clear picture of the creep response of the nanocomposites under investigation can be obtained if we look at their creep compliance at a given time. Figure 9 summarizes the isochronous total compliance and relative components at 2000 s. It can be observed that up to a particle content of 2 vol %, titania nanoparticles are not practically influencing the creep compliance of the HDPE matrix. As the filler content increases, the superior efficiency of untreated titania nanoparticles in reducing the creep compliance is clearly evident, especially at higher filler amounts (5 vol %). In particular, nanocomposites containing 5 vol % TiO_2 showed a 20% reduction of the total creep compliance with respect to the unfilled HDPE matrix. Moreover, it can be noted that a major effect of the nanoparticles is the reduction of the viscoelastic creep compliance component, the elastic one being only slightly reduced. These conclusions are in accordance with the results obtained in quasi-static tensile tests. Even in this case, a more compliant filler–matrix interphase promoted by the organosilane surface functionalization could be responsible for the observed experimental behavior.

Modeling of the creep behavior

The ability to model the viscoelastic response allows a better understanding of the deformation mechanisms and provides a tool to design for long-term load-bearing applications.[33]

A mechanical model that has been successfully applied for the analysis of creep data of various semicrystalline polymers[34] and polymer-based nanocomposites[1] is the Burgers model, which is schematically represented in Figure 10. This is a four-element mechanical model composed of a series combination of the Maxwell and Kelvin models. The creep compliance of this model is given by eq. (4):

$$D(t) = \frac{1}{E_M} + \frac{t}{\eta_M} + \frac{1}{\eta_K}\left[1 - \exp\left(-\frac{E_K}{\eta_K}t\right)\right] \quad (4)$$

where E_M and η_M are the elastic and viscous parameters of the series (Maxwell) elements, E_K and η_K

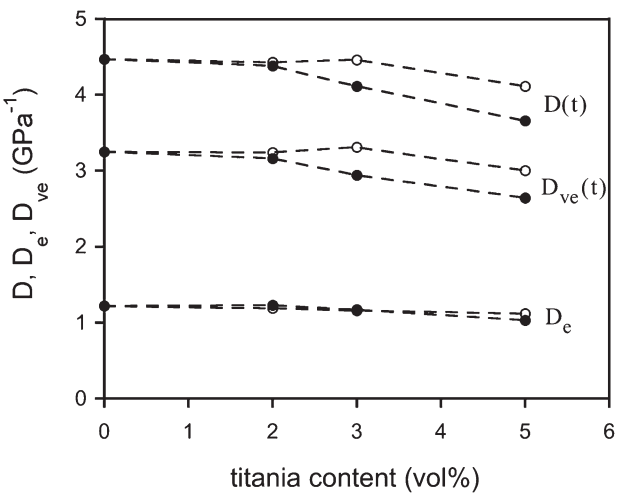

Figure 9 Isochronous creep compliance components at t = 2000 s for nanocomposites containing various amounts of (●) TiO_2 and (○) M-TiO_2 nanoparticles.

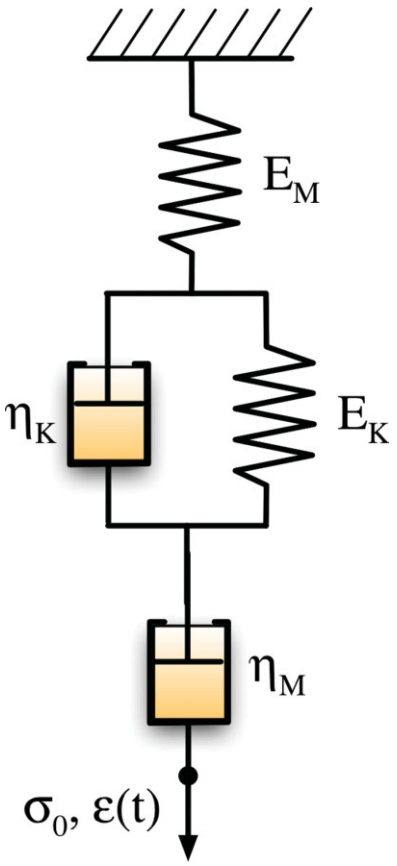

Figure 10 Schematic representation of the Burgers model. σ_0, applied stress; $\varepsilon(t)$, resulting deformation. [Color figure can be viewed in the online issue, which is available at www.interscience.wiley.com.]

represent the elastic and viscous parameters of the parallel (Kevin) elements of the Burgers models indicated in Figure 10.

Another possible approach to creep modeling arises from the consideration that viscoelastic changes in a polymeric material occur with incremental jumps.[33] At a molecular level, this means that there are several segments of macromolecules jumping between positions of relative stability. This approach is based on the Kohlrausch–Williams–Watts (KWW) model and is generally described by a Weibull-like function.[33] The original form of the equation was used for the first time by Kohlraush in the 19th century,[35] whereas its usage in modeling viscoelastic phenomena derives from the work of Williams and Watts on dielectric decay.[36] According to the KWW model, the time-dependent creep compliance can be expressed as follows:

$$D(t) = D_i + D_c\left\{1 - \exp\left[-\left(\frac{t}{t_c}\right)^{\beta_c}\right]\right\} \quad (5)$$

where D_i is the elastic instantaneous component of the creep compliance; D_c is the limiting creep compliance for t approaching infinity; and t_c and β_c are the scale (characteristic time) and shape parameters, respectively. The KWW model has turned out to be very effective in describing relaxation phenomena in various glassy solids[37] and also for modeling the time dependence of the creep compliance of crystalline polymers.[38] We can obtain a power law by expanding the KWW function [eq. (6)] as a series and ignoring all but the first term[39]:

$$D(t) = D_0 + k\left(\frac{t}{t_c}\right)^n \quad (6)$$

This is consistent with Findley's equation[40]:

$$D(t) = D_0 + kt^n \quad (7)$$

where D_0 is the elastic instantaneous creep compliance, k is a coefficient related to the magnitude of the underlying retardation process, and n is an exponent tuning the time dependence of the creep process. D_0 and k are functions of environmental variables,[41] including the temperature and moisture.

As an example, in Figure 11, the creep data of HDPE filled with 5 vol % TiO_2 have been fitted by the functions representing the Burgers [eq. (4)], KWW [eq. (5)], and Findley [eq. (7)] models. The parameters of the models resulting from the best fitting experimental creep data are summarized in Tables IV–VI along with the relative R^2 values. It can be noticed that the Burgers model is only partially able to fit the creep curve, with a somewhat better correspondence to the experimental data at shorter times (<1000 s), the accordance between experimental and fitted data being not fully satisfactory at longer times (average $R^2 = 0.9829$). In fact, the contribution of the dashpot of the Maxwell element (η_M) leads to a linear increase in the creep compliance at long times. Moreover, from a physical point of view, the creep

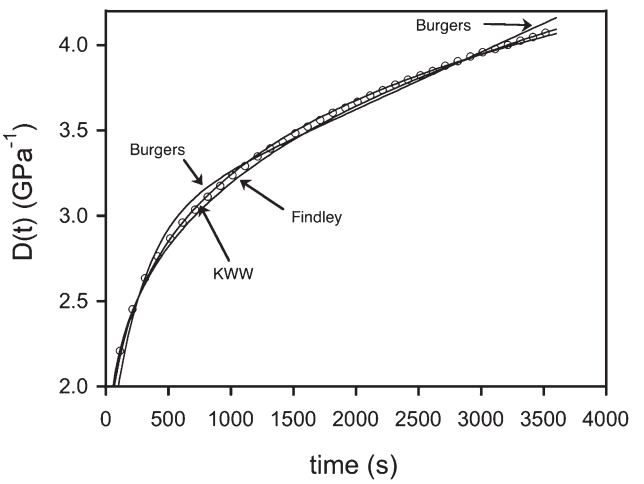

Figure 11 Fitting of the creep data of 95/5 HDPE/TiO_2 (open points) with various models.

TABLE IV
Fitting Parameters According to the Burgers Model for the HDPE and Related Nanocomposites

Material	E_K (GPa)	η_K (GPa·s)	E_M (GPa)	η_M (GPa s)	R^2
HDPE	0.494	87.6	0.820	1818.2	0.9862
98/2 HDPE/TiO_2	0.496	83.7	0.816	1923.1	0.9810
97/3 HDPE/TiO_2	0.526	87.3	0.853	2173.9	0.9833
95/5 HDPE/TiO_2	0.585	99.4	0.973	2439.0	0.9825
98/2 HDPE/M-TiO_2	0.486	80.5	0.839	1923.1	0.9829
97/3 HDPE/M-TiO_2	0.477	81.7	0.865	1886.8	0.9806
95/5 HDPE/M-TiO_2	0.540	93.2	0.896	1960.8	0.9840

deformation associated with this element is irreversible after unloading, and this is not the case under investigation. The fitting definitely improves when we consider the Findley model, for which a somewhat better accordance with the creep data can be reached (average $R^2 = 0.9856$). The best model for fitting creep data appears to be the KWW model, for which a very good accordance between experimental and predicted creep compliances can be observed over the entire experimental range (average $R^2 = 0.9937$).

According to the Burgers model, the sensible reduction of the creep compliance due to the introduction of the nanoparticles is reflected in the marked increase of both the elastic (E_M and E_K) and viscous (η_M and η_K) parameters, especially with untreated titania nanoparticles.

On the basis of the Findley approach, the enhancement of the creep stability induced by the nanoparticles is quantified by the reduction of the exponential parameter n, which is more evident for nanocomposites filled with untreated titania nanoparticles.

More accurate considerations can be inferred from the fitting parameters of the KWW model, for which the best fitting was obtained. The variation of the elastic component of the creep compliance is consistent with the changes observed for the tensile elastic modulus, whereas a significant reduction of the viscous compliance at very long times (D_c) can be easily detected (ca. 30% for the sample filled with 5% TiO_2 with respect of the unfilled material). Although β_c seems to be only slightly affected by the presence of the nanofiller, t_c is markedly reduced for the nanocomposites. From an analytical point of view, t_c represents the time at which the material reaches $1 - 1/e$, that is, about 63% of D_c. This means that nanocomposites deform more rapidly than unfilled HDPE, but to a lower extent. Even in this case, lower t_c values were obtained with untreated nanoparticles with a high filler content.

An analysis of the creep rate can provide some further insight into the deformational behavior of the materials under investigation. Only the KWW and Findley models have been considered because of their better accuracy in fitting the experimental data. A creep rate can be obtained by differentiation of the total creep compliance. According to the KWW model, the following expression of the creep rate can be obtained:

$$\frac{dD(t)}{dt} = \frac{D_c \cdot \beta_c}{(t_c)^{\beta_c}} \exp\left[-\left(\frac{t}{t_c}\right)^{\beta_c}\right] t^{(\beta_c - 1)} \tag{8}$$

As for the Findley model, the expression of the creep rate is given by

$$\frac{dD(t)}{dt} = k\, n\, t^{n-1} \tag{9}$$

The creep rate curves obtained on the basis of the KWW and Findley models are reported in Figures 12 and 13, respectively, for HDPE and relative nanocomposites filled with both untreated and surface-coated nanoparticles at a concentration of 5 vol %. According

TABLE V
Fitting Parameters According to the KWW Model for the HDPE and Related Nanocomposites

Material	D_i (GPa^{-1})	D_c (GPa^{-1})	t_c (s)	β_c	R^2
HDPE	1.220	5.367	2325.6	0.4640	0.9939
98/2 HDPE/TiO_2	1.225	4.658	1515.2	0.4696	0.9932
97/3 HDPE/TiO_2	1.173	4.355	1538.5	0.4666	0.9930
95/5 HDPE/TiO_2	1.028	3.804	1388.9	0.4775	0.9935
98/2 HDPE/M-TiO_2	1.192	4.952	1754.4	0.4645	0.9936
97/3 HDPE/M-TiO_2	1.156	5.044	1724.1	0.4649	0.9942
95/5 HDPE/M-TiO_2	1.117	4.867	2173.9	0.4674	0.9946

TABLE VI
Fitting Parameters According to Findley's Model for the HDPE and Related Nanocomposites

Material	D_e (GPa^{-1})	k ($GPa^{-1} \cdot s^{-n}$)	n	R^2
HDPE	1.220	0.295	0.315	0.9880
98/2 HDPE/TiO_2	1.225	0.336	0.294	0.9839
97/3 HDPE/TiO_2	1.173	0.315	0.293	0.9839
95/5 HDPE/TiO_2	1.028	0.283	0.293	0.9831
98/2 HDPE/M-TiO_2	1.192	0.331	0.299	0.9856
97/3 HDPE/M-TiO_2	1.156	0.340	0.298	0.9862
95/5 HDPE/M-TiO_2	1.117	0.273	0.314	0.9884

to both models, it clearly emerges that titania nanoparticles induce a sensible reduction of the creep rate, which is more pronounced for untreated titania nanoparticles. Moreover, the reduction of the creep compliance is more evident at long creep times (after 1000 s). This result can be explained if we consider that for both models the long-term creep rate depends on parameters that are reduced by the presence of nanoparticles. In fact, according to the KWW model, the long-term creep rate is mostly determined by the parameter β_c, whereas for the Findley approach, the total creep rate is mostly governed by the exponential parameter n.

CONCLUSIONS

Acicular titania nanoparticles with average dimensions of 15 nm × 60 nm were produced by hydrothermal crystallization of $TiOCl_2$. Titania particles were surface-functionalized with $CH_3(CH_2)_{17}SiH_3$ to obtain a more organophilic surface.

HDPE–titania nanocomposites were prepared through the melt compounding process to evaluate the effects of the surface functionalization and the filler amount on their tensile and viscoelastic mechanical responses. Tensile modulus tests evidenced a significant increase in the stiffness of the material, especially for the untreated nanoparticles and for elevated filler loadings. The presence of an organic functionalization on the titania nanoparticles probably leads to a weak interphase between the filler and the matrix, with a negative effect on the stiffness of the nanocomposite. Tensile tests at break confirmed these considerations, the stress at yield being positively affected by the presence of untreated nanoparticles, with only marginal improvements for the surface-treated nanoparticles. In any case, a significant reduction of the strain at break can be detected, especially for higher filler loadings.

Creep tests showed a pronounced decrease in the creep compliance for both the elastic and viscous components, especially with untreated particles at a concentration of 5 vol %. The creep compliance reduction induced by the surface-modified titania nanoparticles is lower, probably because of the presence of a softer interphase.

Various creep models were adopted to analyze the creep data. A good fitting of the experimental data can be obtained with the KWW model and Findley equation. A substantial reduction of the creep rate can be estimated for long creep times because of the presence of untreated titania nanoparticles.

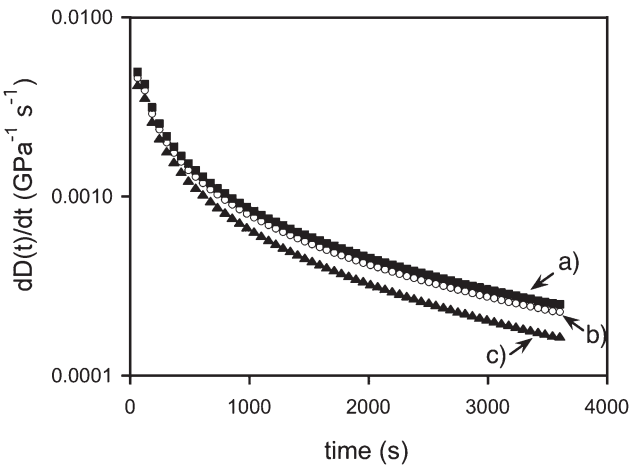

Figure 12 Creep rate curves according to the KWW model: (a) HDPE, (b) 95/5 HDPE/M-TiO_2, and (c) 95/5 HDPE/TiO_2.

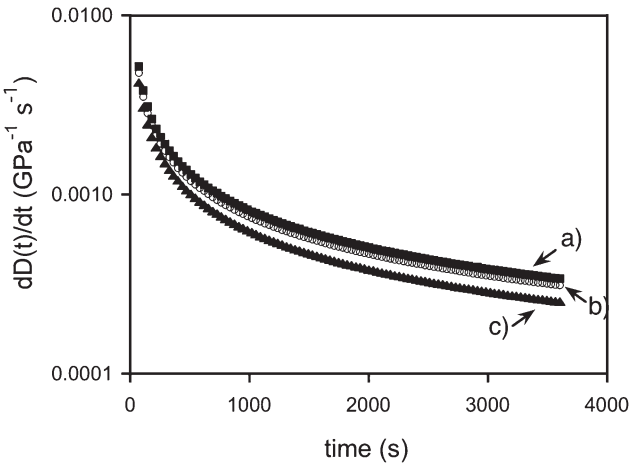

Figure 13 Creep rate curves according to the Findley model: (a) HDPE, (b) 95/5 HDPE/M-TiO_2, and (c) 95/5 HDPE/TiO_2.

The authors thank Rubens A. Bonacorsi for his support of the experimental work.

References

1. Pegoretti, A. In Nano- and Micromechanics of Polymer Blends and Composites; Karger-Kocsis, J.; Fakirov, S., Eds.; Hanser: Munich, to appear.
2. Hussain, F.; Hojjati, M.; Okamoto, M.; Gorga, R. E. J Compos Mater 2006, 1511, 40.
3. Lazzeri, A.; Zebarjad, S. M.; Pracella, M.; Cavalier, K.; Rosa, R. Polymer 2005, 827, 46.

4. Ou, Y. C.; Yang, F.; Yu, Z. Z. J Polym Sci Part B: Polym Phys 1998, 789, 36.
5. Kolarik, J.; Fambri, L.; Pegoretti, A.; Penati, A.; Goberti, P. Polym Eng Sci 2002, 161, 42.
6. Kolarik, J.; Pegoretti, A.; Fambri, L.; Penati, A. J Appl Polym Sci 2003, 641, 88.
7. Starkova, O.; Yang, J.; Zhang, Z. Compos Sci Technol 2007, 2691, 67.
8. Yang, J. L.; Zhang, Z.; Schlarb, A. K.; Friedrich, K. Polymer 2006, 6745, 47.
9. Yang, J. L.; Zhang, Z.; Schlarb, A. K.; Friedrich, K. Polymer 2006, 2791, 47.
10. Zhang, Z.; Yang, J. L.; Friedrich, K. Polymer 2004, 3481, 45.
11. Siengchin, S.; Karger-Kocsis, J.; Thomann, R. J Appl Polym Sci 2007, 2963, 105.
12. Bondioli, F.; Dorigato, A.; Fabbri, P.; Messori, M.; Pegoretti, A. Polym Eng Sci 2008, 448, 48.
13. Pegoretti, A.; Dorigato, A.; Penati, A. Express Polym Lett 2007, 123, 1.
14. Pegoretti, A.; Accorsi, M. L.; DiBenedetto, A. T. J Mater Sci 1996, 6145, 31.
15. Gopakumar, T. G.; Lee, J. A.; Kontopoulou, M.; Parent, J. S. Polymer 2002, 5483, 43.
16. Osman, A. M.; Rupp, J. E. P.; Suter, U. W. Polymer 2005, 8202, 46.
17. Ranade, A.; Nayak, K.; Fairbrother, D.; D'souza, N. A. Polymer 2005, 7323, 46.
18. Bonamartini Corradi, A.; Bondioli, F.; Ferrari, A. M.; Romagnoli, M. Submitted.
19. Fadeev, A. Y.; Helmy, R.; Marcinko, S. Langmuir 2002, 7521, 18.
20. de Farias, R. F.; Airoldi, C. J Therm Anal Calorim 1998, 751, 53.
21. Bondioli, F.; Dorigato, A.; Fabbri, P.; Ferrari, A. M.; Messori, M.; Pegoretti, A. Presented at NSTI Nanotech Ventures, Boston, MA, June 2008.
22. Helmy, R.; Fadeev, A. Y. Langmuir 2002, 8924, 18.
23. Nielsen, L. E.; Landel, R. F. Mechanical Properties of Polymers and Composites; Marcel Dekker: New York, 1994.
24. Cassagnau, P. Polymer 2008, 2183, 49.
25. Durmus, A.; Kasgoz, A.; Macosko, C. W. Polymer 2007, 48, 4492.
26. Kolarik, J.; Pegoretti, A. Polymer 2006, 346, 47.
27. Hotta, S.; Paul, D. R. Polymer 2004, 7639, 45.
28. Morawiec, J.; Pawlak, A.; Slouf, M.; Galeski, A.; Piorkowska, E.; Krasnikowa, N. Eur Polym J 2005, 1115, 41.
29. Tanniru, M.; Yuan, Q.; Misra, R. D. K. Polymer 2006, 2133, 47.
30. Crawford, R. Plastics Engineering; Pergamon: Oxford, 1999.
31. Lakes, R. S. Viscoelastic Solids; CRC: Boca Raton, FL, 1999.
32. Ward, I. M.; Hadley, D. W. An Introduction to the Mechanical Properties of Solid Polymers; Wiley: Chichester, United Kingdom, 1993.
33. Fancey, K. S. J Mater Sci 2005, 4827, 40.
34. Holmes, D. W.; Loughran, J. G.; Suehrcke, H. Mech Time-Dependent Mater 2006, 281, 10.
35. Kohlrausch, F. Ann Phys 1863, 337, 119.
36. Williams, G.; Watts, D. C. Trans Faraday Soc 1970, 80, 66.
37. Palmer, R. G.; Stein, D. L.; Abrahams, E.; Anderson, P. W. Phys Rev Lett 1984, 958, 53.
38. Fancey, K. S. J Polym Eng 2001, 489, 21.
39. Tomlins, P. E. Polymer 1996, 3907, 37.
40. Findley, W. N. Polym Eng Sci 1987, 582, 27.
41. Lietz, S.; Yang, J. L.; Bosch, E.; Sandler, J. K. W.; Zhang, Z.; Altstadt, V. Macromol Mater Eng 2007, 23, 292.